Journal of Nuclear Materials 408 (2011) 153–160

Contents lists available at ScienceDirect

Journal of Nuclear Materials

journal homepage: www.elsevier.com/locate/jnucmat

Radiation-induced stress relaxation in high temperature water of type 316L stainless steel evaluated by neutron diffraction

Y. Ishiyama [a,*], R.B. Rogge [b], M. Obata [c]

[a] Nippon Nuclear Fuel Development Co., Ltd., Narita-cho, Oarai-machi, Higashi-Ibaraki-gun, Ibaraki 311-1313, Japan
[b] National Research Council Canada, Chalk River Laboratories, Chalk River, Ontario, Canada KOJ 1JO
[c] Toshiba Corp., 8 Shinsugita-cho, Isogo-ku, Yokohama 235-8523, Japan

ARTICLE INFO

Article history:
Received 9 June 2010
Accepted 10 November 2010

ABSTRACT

Weld beads on plate specimens made of type 316L stainless steel were neutron-irradiated up to about 2.5×10^{25} n/m^2 ($E > 1$ MeV) at 561 K in the Japan Material Testing Reactor (JMTR). Residual stresses of the specimens were measured by the neutron diffraction method, and the radiation-induced stress relaxation was evaluated. The values of σ_x residual stress (transverse to the weld bead) and σ_y residual stress (longitudinal to the weld bead) decreased with increasing neutron dose. The tendency of the stress relaxation was almost the same as previously published data, which were obtained for type 304 stainless steel. From this result, it was considered that there was no steel type dependence on radiation-induced stress relaxation. The neutron irradiation dose dependence of the stress relaxation was examined using an equation derived from the irradiation creep equation. The coefficient of the stress relaxation equation was obtained, and the value was 1.4 ($\times 10^{-6}$/MPa/dpa). This value was smaller than that of nickel alloy.

1. Introduction

Numerous stress corrosion crack (SCC) growth examinations using neutron-irradiated specimens have been performed and their results reported [1–4]. SCC growth occurs around a welded zone because of its residual tension stress, so that stress is one of the important factors for evaluation of SCC growth. Therefore, stress evaluation is important for accurate prediction of SCC growth and for evaluation of health of nuclear reactor components.

On the other hand, influence of stress relaxation caused by neutron irradiation on SCC growth has not been considered in evaluations to date because of fewer available data. Causey, alone [5,6] and with co-authors [7,8], has extensively investigated the stress relaxation and creep under fast neutron irradiation of austenitic stainless steels and other metals using the bent-beam method. Foster et al. [9–11] have evaluated irradiation creep of austenitic stainless steels using bent beams and pressurized tubes to predict their stress relaxation behaviors from the obtained creep data. Ishiyama et al. [12] have performed bent beam tests and C-ring tests, in which different stress ranges were applied, to evaluate the effects of plastic deformation and difference of applied stress on radiation-induced relaxation in some types of austenitic stainless steels at 561 K. All these studies treated the radiation-induced relaxation of mechanically applied stress under uni-axial or bi-axial conditions. However, residual tension stress in welded components is generated by constraining the volume change during the welding heat cycle; consequently, there is a possibility that its relaxation behavior is different from that of mechanically applied stress.

The objectives of this study are to obtain radiation-induced stress relaxation data in welded type 316L stainless steel and to evaluate the radiation-induced stress relaxation behavior.

2. Experimental procedure

2.1. Specimen preparation and neutron irradiation

The specimens were made of type 316L stainless steel having the chemical composition shown in Table 1. The specimens were solution-heat treated at 1303 K for 0.5 h and quenched in water. Thereafter one-pass welding beads were formed at the center on the specimens under the mechanical constraint condition. A schematic illustration of a specimen and measurement directions (x, y, z) are shown in Fig. 1.

Neutron irradiation was carried out in the Japan Materials Testing Reactor (JMTR) of the Japan Atomic Energy Agency (JAEA). The specimens were irradiated in high temperature water at 561 K. Three neutron fluences were used: 5.3×10^{24}, 1.2×10^{25} and 2.5×10^{25} n/m^2 ($E > 1$ MeV). The neutron fluence of each specimen was converted to irradiation dose (dpa) by a calculation based on its chemical composition and irradiation history. The neutron doses were 0.9, 1.9 and 4.1 dpa, respectively.

* Corresponding author. Tel.: +81 29 266 2131; fax: +81 29 266 2589.
E-mail address: ishiyama@nfd.co.jp (Y. Ishiyama).

0022-3115/$ - see front matter © 2010 Elsevier B.V. All rights reserved.
doi:10.1016/j.jnucmat.2010.11.023

Table 1
Chemical composition of specimens (mass%).

C	Si	Mn	P	S	Ni	Cr	Mo	Co	Fe
0.008	0.43	0.83	0.23	0.001	12.55	17.54	2.11	0.02	bal.

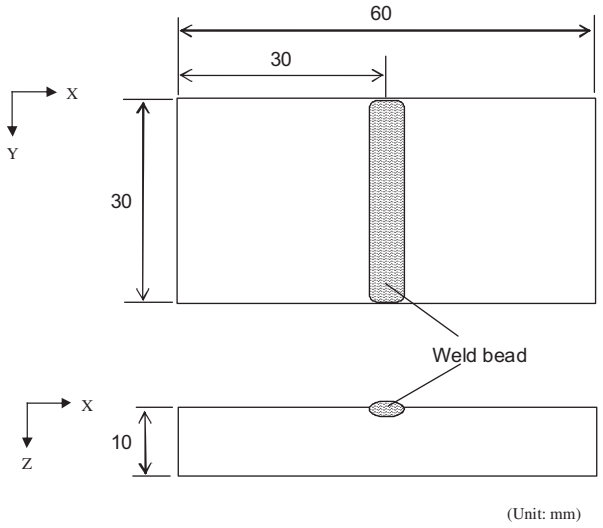

Fig. 1. Schematic illustration of welded type 316L specimen.

2.2. Stress relaxation measurement by neutron diffraction method

Residual stresses of the specimens were measured by the neutron diffraction method after neutron irradiation. Neutrons are directed towards the measurement location within the specimen where they are diffracted from the lattice planes of the crystallites that form the material. The angle (2θ) at which the neutrons are diffracted depends on the wavelength of the incident neutron beam and the spacing between the lattice planes, through Bragg's law:

$$\lambda = 2d\sin(\theta), \tag{1}$$

where θ is Bragg angle, λ is wavelength of the incident neutron beam, and d is lattice spacing. The lattice strain is the fractional change in the lattice spacing with reference to the *stress-free* lattice spacing, that is

$$\varepsilon = \frac{d - d_0}{d_0}, \tag{2}$$

where ε is lattice strain and d_0 is lattice spacing under the *stress-free* condition. The three residual stress components can then be calculated from the three measured strain components using the Generalized Hooke's Law:

$$\sigma i = \frac{E}{1+v}\left[\varepsilon i + \frac{v}{1-2v}(\varepsilon x + \varepsilon y + \varepsilon z)\right], (i = x, y, z), \tag{3}$$

where E is the Young's modulus and v is the Poisson ratio. In this measurement, material constants of 193.3 GPa for Young's modulus and 0.3 for the Poisson ratio, and the γ phase (311) lattice plane were used.

Neutron diffraction measurements were performed using the National Research Universal (NRU) reactor of the National Research Council of Canada (NRC). A schematic drawing of the neutron diffractometer geometry is shown in Fig. 2. The thermal neutron beam emitted by the reactor was diffracted from the (511) plane of a single-crystal germanium monochromator. The wavelength of the monochromatic neutron beam was 0.153 nm. The specimens were irradiated by the monochromatic neutron beam through the incident slit (3 mm width), and then the diffracted beam on the γ phase (311) plane was passed though another slit (3 mm width and 3 mm height); the nominal gage volume was $3 \times 3 \times 3$ mm. The diffraction peak profile of the neutron beam was measured by a ^{3}He multi-wire detector. To reduce the influence of γ rays from the radioactivated specimen, a specially designed shielded container was fabricated. The specimen was moved by a computer-controlled translation and rotation system to position the instrumental gage volume at locations of interest within the specimen. The specimens were oscillated ±1.5° during all measurements.

Measurement locations in the specimens are shown in Fig. 3. All measurements were made in the cross section perpendicular to the weld line and approximately mid-length along the 30 mm dimension of the specimen. Three different distance locations from the welded surface, at 1/4-, 1/2- and 3/4-thickness of the specimen, were measured.

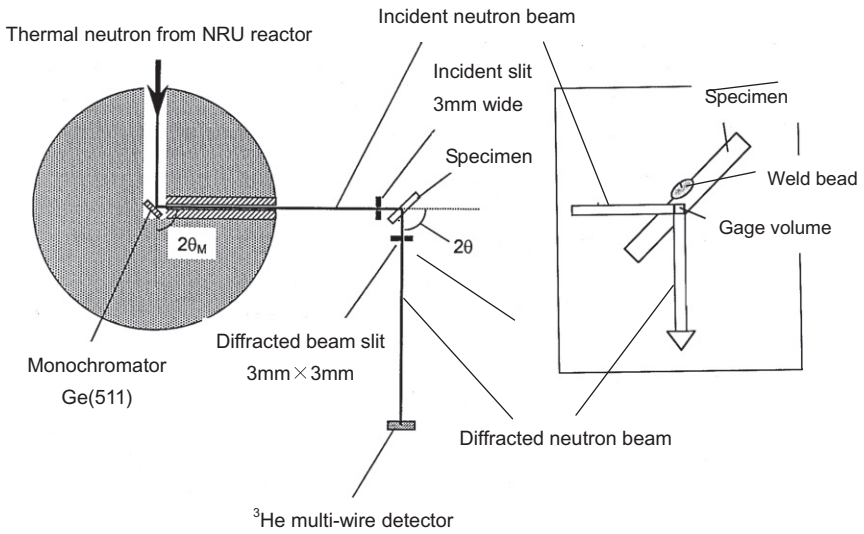

Fig. 2. Schematic drawing of neutron diffractometer geometry.

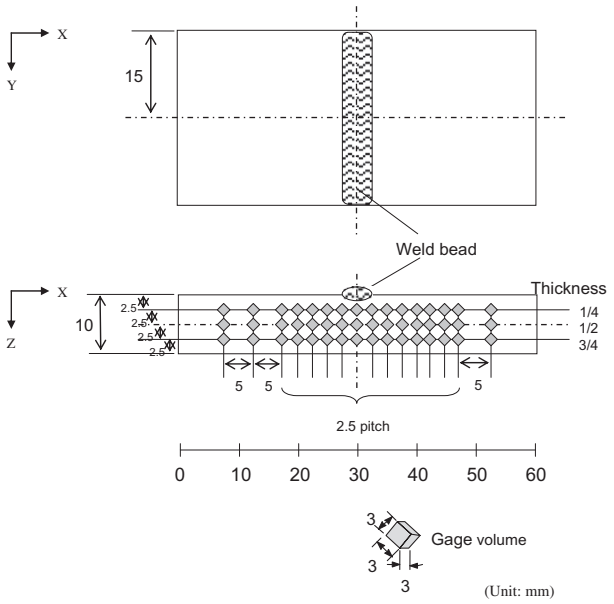

Fig. 3. Measurement locations on the welded type316L specimens.

3. Results

Residual stress distribution measurements were made on three irradiated specimens and one un-irradiated specimen. The measurement results are shown in Figs. 4–6. Comparison of residual stress distributions between irradiated and un-irradiated specimens at 1/4-thickness is shown in Fig. 4. The distribution of σ_x (perpendicular to the weld direction) is shown in Fig. 4a, the distribution of σ_y (parallel to the weld direction) is shown in Fig. 4b and the distribution of σ_z (normal to the plate) is shown in Fig. 4c. In the same way, the results at the 1/2-thickness are shown in Fig. 5 and the results at the 3/4-thickness are shown in Fig. 6. The stress distributions of σ_x and σ_y at the 1/4- and 1/2-thickness are clear. The σ_x distribution shows a shape that has a tension stress peak at the weld bead position, and the σ_y distribution shows a shape that has a tension stress peak at the weld position and compression stress peak on both sides of the weld bead. For the σ_z, however, a clear distribution is not observed at every thickness. Also, clear stress distributions are not observed in every direction stress (σ_x, σ_y, σ_z) at the 3/4-thickness. Regarding comparison of the irradiation effects on the stress distributions of σ_x and σ_y at the 1/4- and 1/2-thickness, for which the distributions are clear, there is no remarkable difference between the un-irradiated and 1.2×10^{25} n/m^2 irradiated specimens. But remarkable stress relaxation is observed in the 2.5×10^{25} n/m^2 irradiated specimen. Irradiation fluence dependence on stress relaxation was evaluated for σ_x and σ_y at 1/4- and 1/2-thickness which had clear stress distributions. Prior to the evaluation, the stress distributions were fitted by a Gaussian distribution curve because the data were scattered. The fitting result of the 2.5×10^{25} n/m^2 irradiated specimen is not good because the data were scattered widely, especially for σ_x at 1/4-thickness. On the other hand, the fitting results for the un-irradiated specimen and the 5.3×10^{24} n/m^2 and 1.2×10^{25} n/m^2 irradiated specimens are good. Irradiation fluence dependences of tension and compression peak stress values of these fitted curves at 3/4- and 1/2-thickness are shown in Figs. 7 and 8. In the case of tension stress, both σ_x and σ_y decrease with increasing irradiation fluence at 3/4- and 1/2-thickness. On the other hand, no clear irradiation fluence dependence is observed in compression stress σ_y at 3/4- and 1/2-thickness. To evaluate the degree of stress relaxation, the vertical axis was defined as

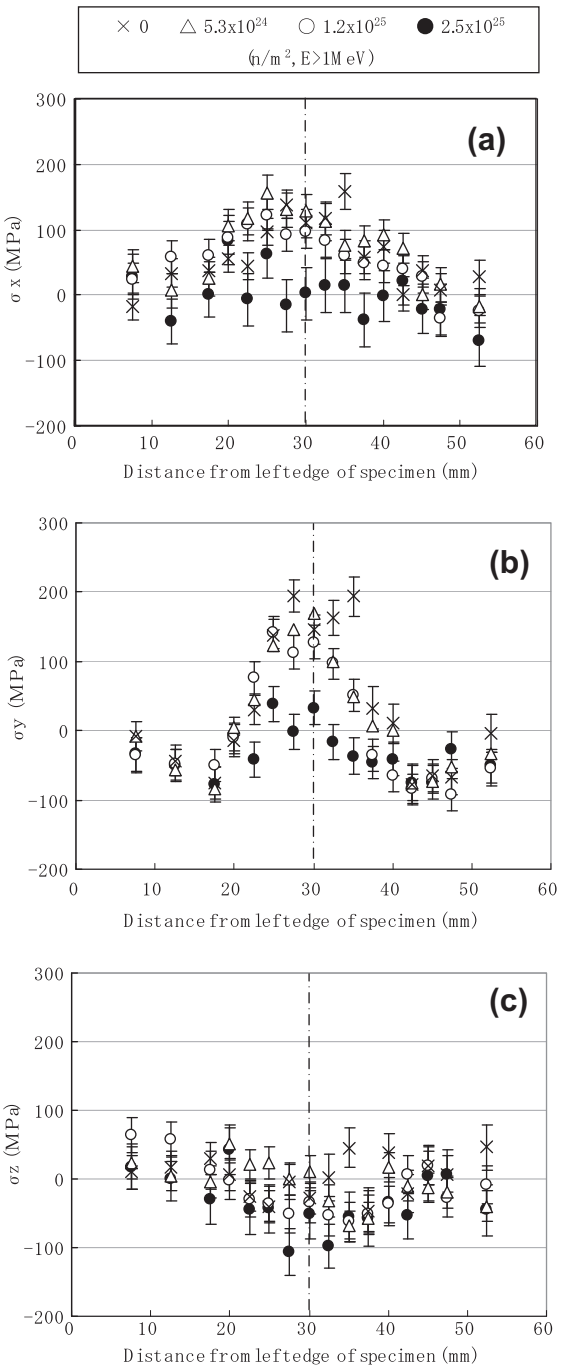

Fig. 4. Comparison of residual stress distributions between un-irradiated and irradiated specimens at 1/4-thickness: (a) σ_x, (b) σ_y and (c) σ_z.

the stress ratio of the irradiated specimen to the un-irradiated specimen. The respective results at 3/4- and 1/2-thickness are shown in Figs. 9 and 10. In the case of tension stress, the stress is relaxed to about 0.1 of the stress ratio at 2.5×10^{25} n/m^2. On the other hand, the ratio of compression stress is almost 1, independent of irradiation fluence, and stress relaxation is not observed.

4. Discussion

Comparison of stress relaxation results with literature data [13] is shown in Fig. 11. Stress is the peak value of the stress distribution. The reference data were obtained for type 304 stainless steel

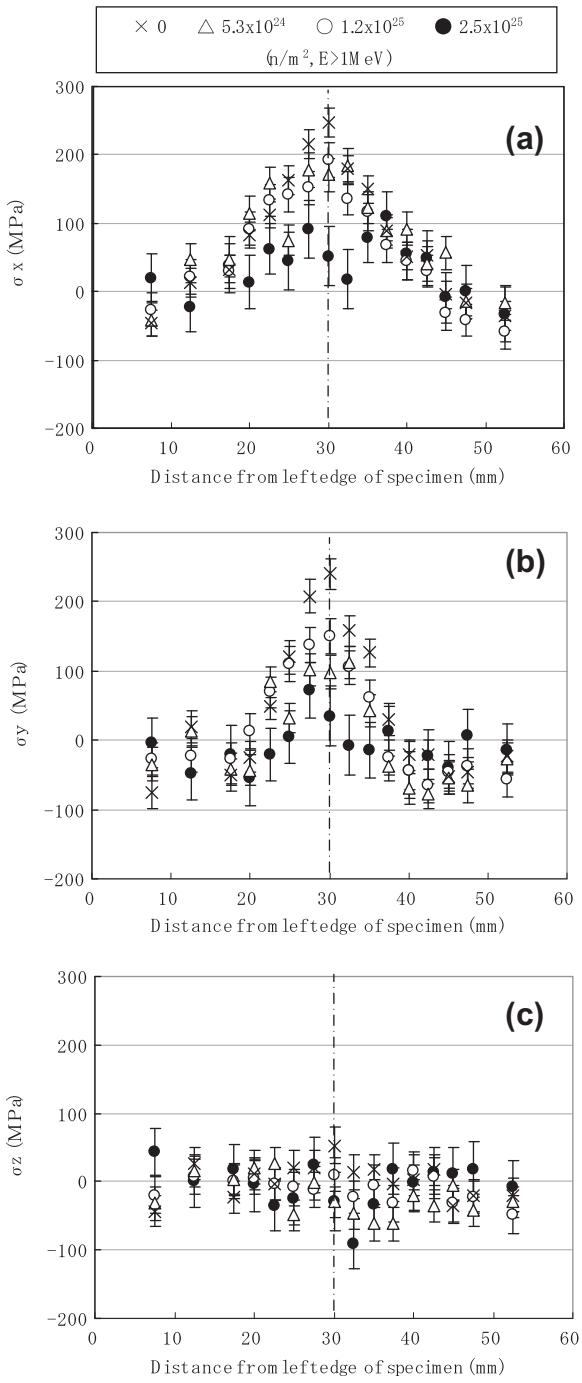

Fig. 5. Comparison of residual stress distributions between un-irradiated and irradiated specimens at 1/2-thickness: (a) σ_x, (b) σ_y and (c) σ_z.

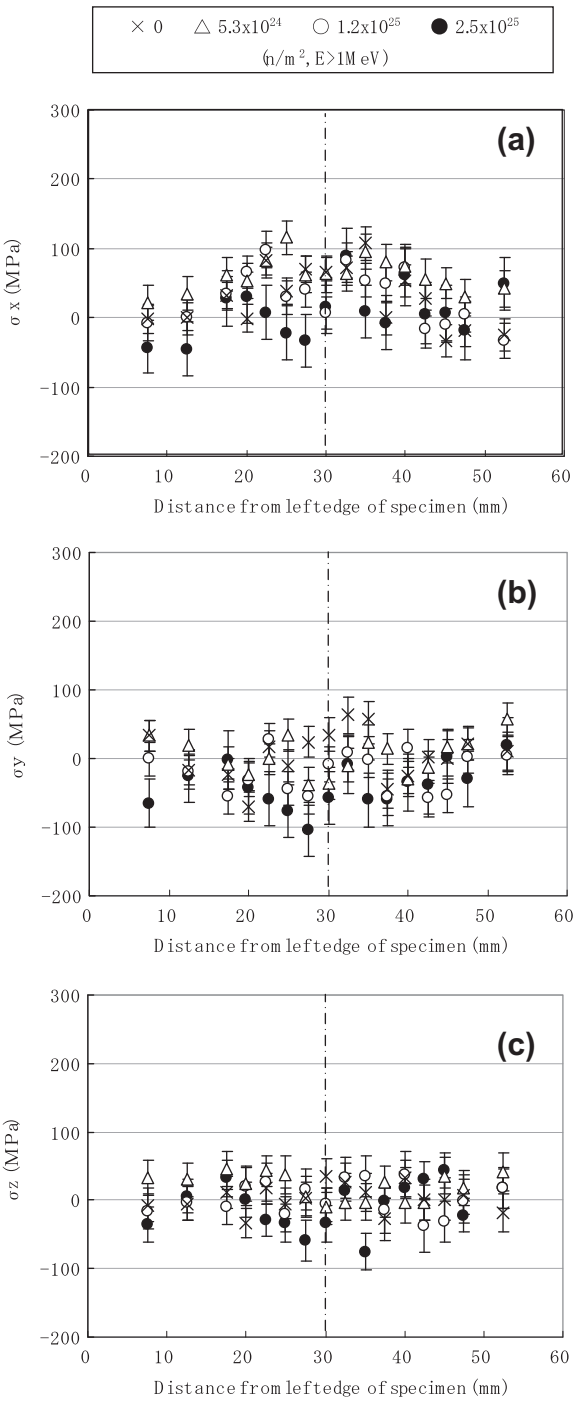

Fig. 6. Comparison of residual stress distributions between un-irradiated and irradiated specimens at 3/4-thickness: (a) σ_x, (b) σ_y and (c) σ_z.

specimens that had been irradiated in high temperature inert gas at 561 K in the JMTR. The reported data were obtained at 1/2-thickness, so that comparison was made to the same 1/2-thickness data in this study. Furthermore, irradiation fluence (n/m^2) values of the present study were converted into irradiation dose (dpa). Tension stress (σ_x and σ_y) relaxation behavior shows the same irradiation dose dependence property for both this study's data and the reference data. These data can be fitted by one trend line, except for the data at 4 dpa of this study. The measured stress values of the 4 dpa irradiated specimen are scattered widely and have a large margin of error. This scatter is attributed to γ rays from the high neutron-irradiated specimen. The specimen is set in the shielded container to reduce the γ rays incident on the detector. But, in case of high neutron-irradiated specimen, amount of γ rays which pass through the shielded container and incident on the detector increase. This causes electrical noise and makes measured stress values scattered. It is considered that therefore the 4 dpa data falls below the trend line. On the other hand, the compression stress (σ_y) of the literature data is relaxed with increasing irradiation dose, but compression stress (σ_y) of this study does not show clear stress relaxation dependence on irradiation dose. Except for the un-irradiated specimen data, the stress relaxation dependence on irradiation dose is almost the same as the literature data. In Ref. [13], stress ratio is defined as the stress ratio of the data after irradiation to the data before irradiation. On the other hand, stress

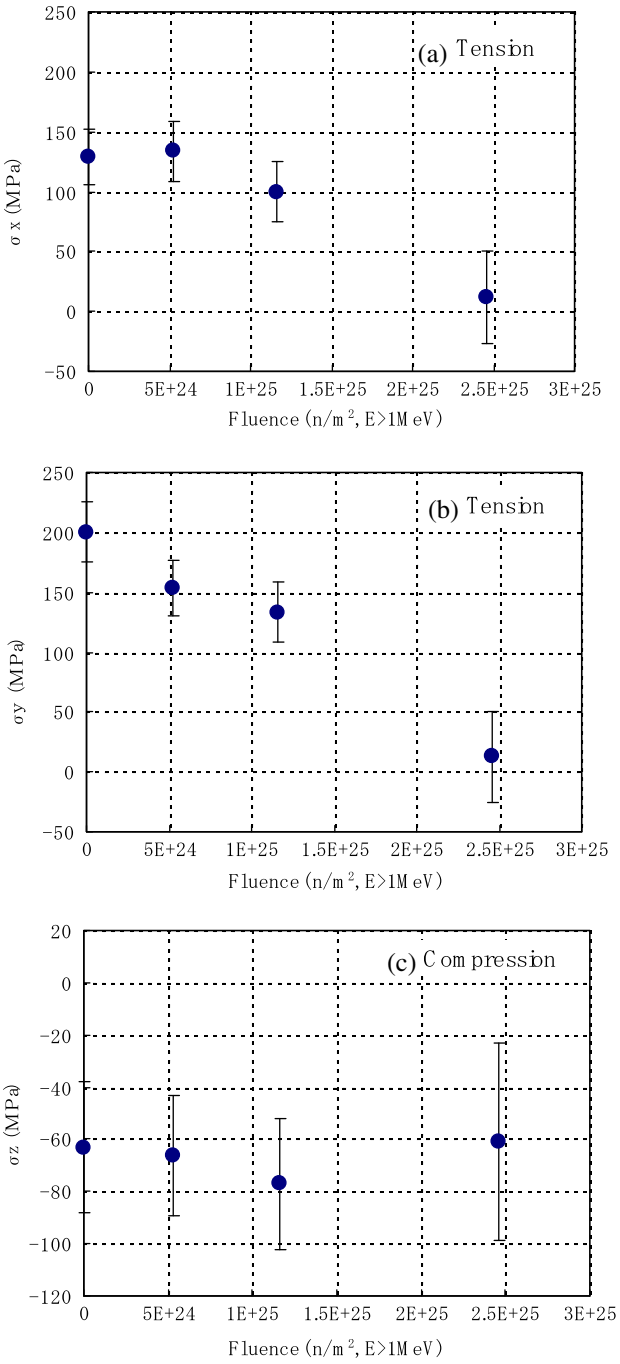

Fig. 7. Irradiation fluence dependence of peak stress at 3/4-thickness: (a) σ_x : tension, (b) σ_y : tension and (c) σ_y: compression.

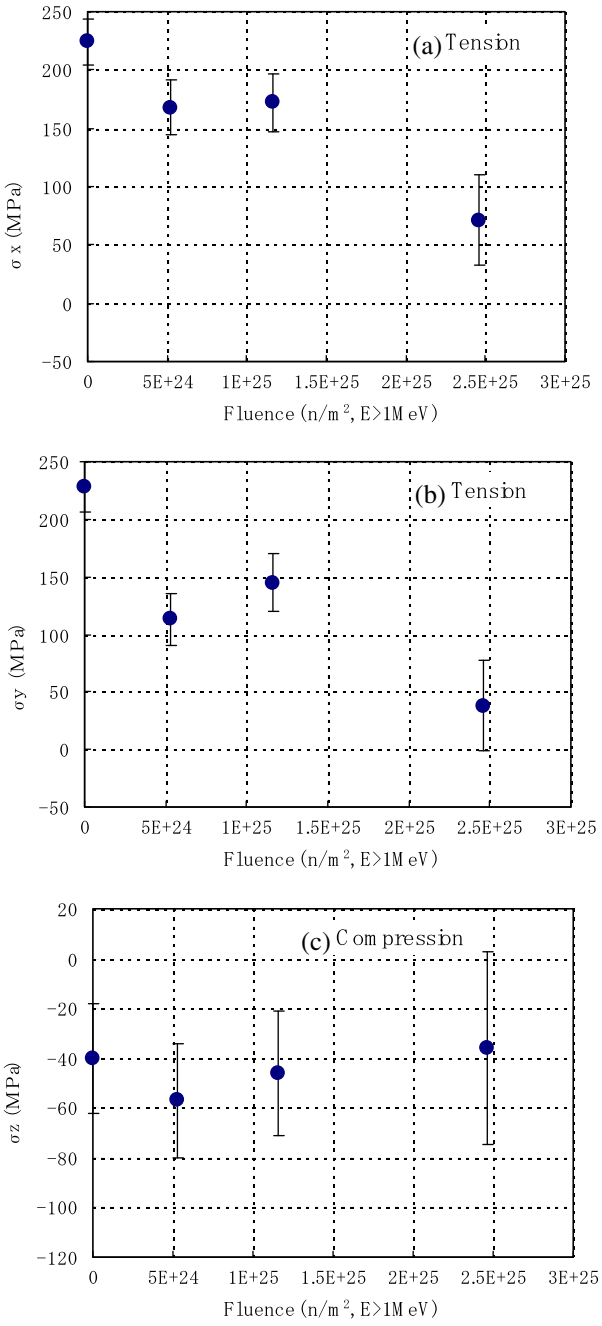

Fig. 8. Irradiation fluence dependence of peak stress at 1/2-thickness: (a) σ_x : tension, (b) σ_y : tension and (c) σ_y : compression.

ratio is defined as the stress ratio of the irradiated specimen to the un-irradiated specimen in this study. All the specimens used in this study have the same manufacturing and welding history, and the stress distributions are almost the same, but not completely. This is considered as one reason why the compression stress does not show clear stress relaxation dependence on irradiation dose in this study. As a general trend, stress relaxation dependence on irradiation dose of literature data and this study are almost the same. Therefore, it is considered that irradiation stress relaxation is not dependent on stainless steel type and irradiation environment (high temperature water or inert gas).

An equation of radiation-induced stress relaxation has been proposed [9]:

$$\sigma/\sigma_0 = exp\{-E[A_1(1 - exp(-A_2\phi)) + A_3\phi]\}, \quad (3)$$

where σ is stress, E is Young's modulus, φ is radiation dose, and A_1, A_2 and A_3 are coefficients. This equation was derived from the radiation-induced creep equation considering transient creep and no swelling condition [14]. If only steady state creep contributed to radiation-induced stress relaxation, the equation of radiation-induced stress relaxation should be expressed as the following equation.

$$\sigma/\sigma_0 = exp(-EA_3\phi). \quad (4)$$

In this study, transient relaxation appears to be very small and can be ignored, therefore the stress relaxation behavior can be evaluated using Eq. (4). As shown in the above, the irradiation dose dependence of tension stress (σ_x and σ_y) relaxation of this study

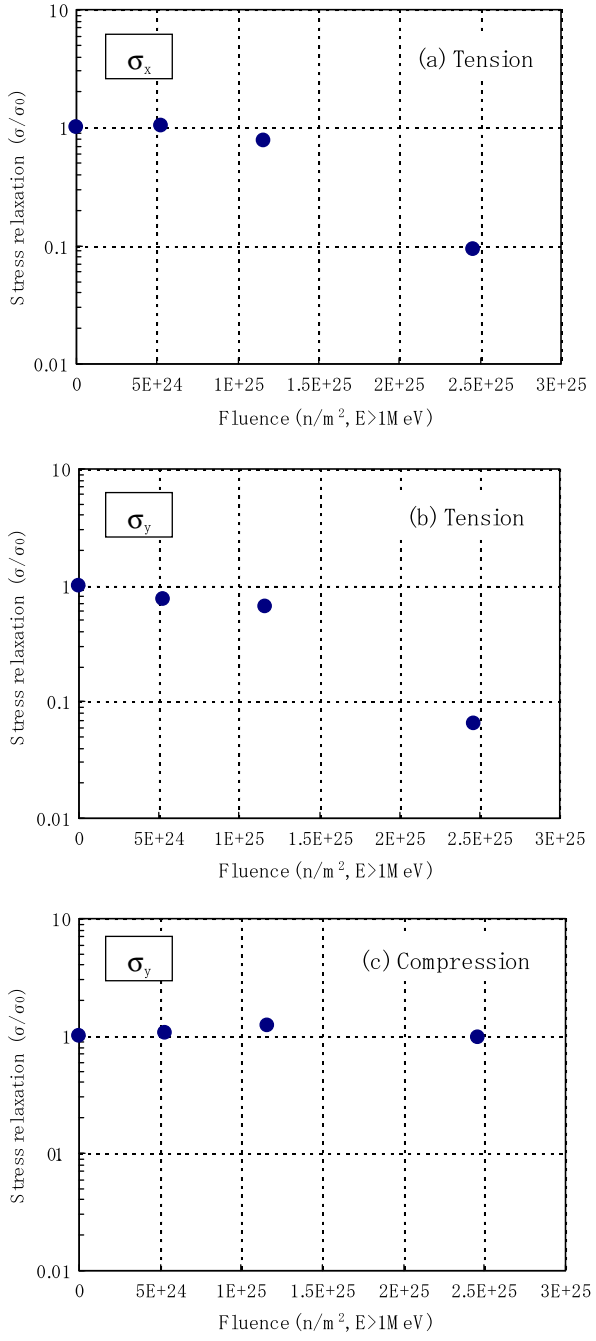

Fig. 9. Irradiation fluence dependence of peak stress relaxation at 3/4-thickness: (a) σ_x : tension, (b) σ_y : tension and (c) σ_y : compression.

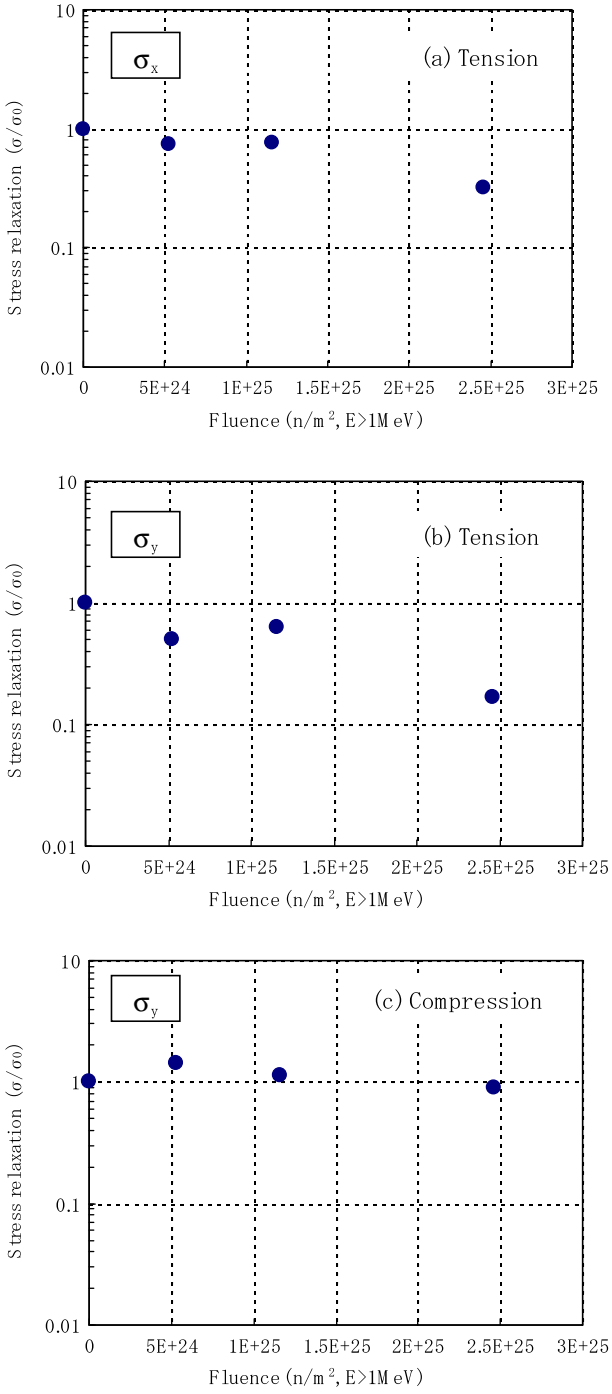

Fig. 10. Irradiation fluence dependence of peak stress relaxation at 1/2-thickness: (a) σ_x : tension, (b) σ_y : tension and (c) σ_y : compression.

and the literature were almost the same so all these data were plotted in Fig. 12. These data were regression approximation fitted by Eq. (4). The value of E was 194 GPa. Two fitting cases were used. The solid line is the result which used all data. In this case, the A_3 coefficient is 1.8 ($\times 10^{-6}$/MPa/dpa). The dotted line is the result which omitted the 1/4-thickness data of the 4 dpa specimen, because these data slightly deviated from the overall trend. In this case, the A_3 coefficient is 1.4 ($\times 10^{-6}$/MPa/dpa). The latter case is considered to be more appropriate, because the 4 dpa data were scattered and 1/4-thickness data deviated from the overall trend.

This coefficient value 1.4 ($\times 10^{-6}$/MPa/dpa) was compared with published data. Ishiyama et al. [12] performed radiation-stress relaxation experiments for type 304 and type 316L stainless steels by the C-ring method and bent method at 561 K. They obtained A_3 coefficients having values of 0.6–1.8 ($\times 10^{-6}$/MPa/dpa). Causey et al. [8] performed radiation-stress relaxation experiments for type 304 stainless steel by the bent method at 570 K. They obtained the A_3 coefficient as 1.1 ($\times 10^{-6}$/MPa/dpa). From these results, the A_3 coefficient of austenitic stainless steels is considered to be around 1.0 ($\times 10^{-6}$/MPa/dpa). Causey et al. [8] also did radiation-stress relaxation experiments for nickel and Zircaloy-2 by the bent method at 570 K, and obtained A_3 coefficients of 8 ($\times 10^{-6}$/MPa/dpa) for nickel and 0.4 ($\times 10^{-6}$/MPa/dpa) for Zircaloy-2. These A_3 coefficients are summarized in Table 2. The literature values, obtained by the bent method, were obtained from the steady state region. In the case of applying a load which causes

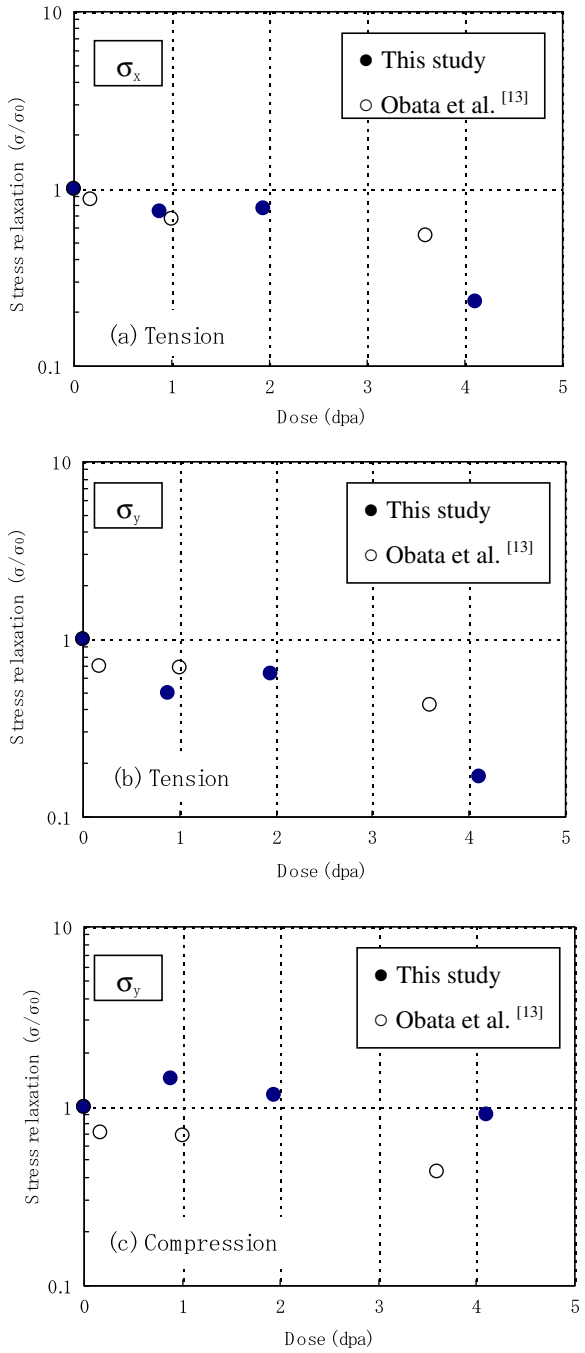

Fig. 11. Comparison of irradiation fluence dependence of peak stress relaxation at 1/2-thickness: (a) σ_x : tension, (b) σ_y : tension and (c) σ_y : compression.

plastic deformation, a transient region can be observed in the initial stage of irradiation. However, it has been reported that stress relaxation behavior of the steady state, following the transient region, shows almost the same behavior as only the steady state observation condition [12]. And it has been reported from an irradiation creep test that the transient region behavior differs according to the magnitude of plastic deformation, but the steady state behavior is almost constant, independent of the magnitude of plastic deformation [14]. From the above, it is considered that comparison of A_3 coefficient value obtained from steady state region is appropriate. As shown in Table 2, the A_3 coefficient of nickel is 8 ($\times 10^{-6}$/MPa/dpa). This value is about 8 times larger than the value of austenitic stainless steel. On the other hand, A_3 coefficient of

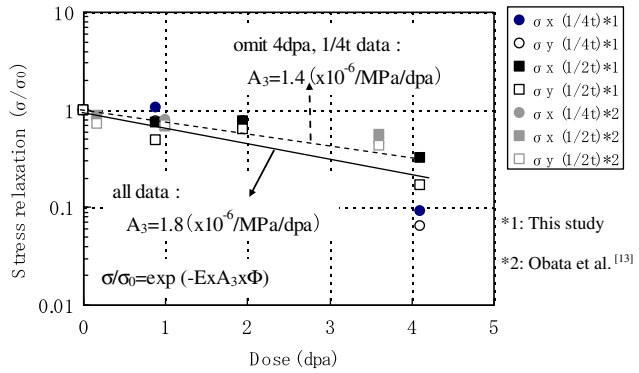

Fig. 12. Equation of radiation-induced stress relaxation obtained by regression approximation fit for the results of this study and literature data [13].

Table 2
Comparison of stress relaxation coefficient of various materials evaluated by examination results.

Material	Temperature (K)	Coefficient A_3 ($\times 10^{-6}$/MPa/dpa)	Test method (specimen type)	Refs.
Austenitic stainless steels	561	1.4	Weld	This study
	561	0.6– 2	C-ring	[12]
	561	0.8–1.8	Bent	[12]
	570	1.1	Bent	[8]
Nickel	570	8	Bent	[8]
Zircaloy-2	570	0.4	Bent	[8]

Zircaloy-2 is 0.4 ($\times 10^{-6}$/MPa/dpa), and this is about half of the value of austenitic stainless steel. These show that stress relaxation of nickel is larger than that of austenitic stainless steel and stress relaxation of Zircaloy-2 is smaller than that of austenitic stainless steel. It is not clear why these A_3 coefficients vary among the materials. But considering the irradiation stress relaxation mechanism [15–17], it is likely that this difference is caused by a difference in dislocation mobility (kinetics, migration energy, interaction with point defects, etc.). In addition, difference of crystal system is also considered to be one of the reasons (austenitic stainless steel and nickel; f. c. c, Zircaloy-2; h. c. p). As concerns nickel, crystal system is same as austenitic stainless steel, but A_3 coefficient value is larger. As one of the reasons, ^{59}Ni effects and bubble-enhanced stress relaxation are considered. Garner et al. have shown that extra dpa generated by ^{59}Ni reactions enhanced irradiation creep [18–20], and helium and hydrogen bubbles generated by ^{59}Ni reactions enhanced irradiation creep [21–22].

From the above, it is considered that the A_3 coefficient (obtained from the steady state region) is not dependent on the experimental method but varies among materials.

5. Conclusions

Radiation-induced stress relaxation of welded type 316L stainless steel specimens was investigated by using the neutron diffraction method. σ_x and σ_y residual tension stress decreased with increasing neutron dose. The tendency of the stress relaxation was almost the same as in literature data, which were obtained for type 304 stainless steel. From this result, it was considered that steel type dependence on radiation-induced stress relaxation did not occur. On the other hand, stress relaxation dependence on irradiation dose in compression stress was not clear. The irradiation dose dependence of the stress relaxation was examined using the radiation-induced stress relaxation Eq. (4) derived from the irradiation creep equation.

$$\sigma/\sigma_0 = exp(-EA_3\phi). \quad (4)$$

The coefficient A_3 of the stress relaxation equation was obtained as 1.4 ($\times 10^{-6}$/MPa/dpa). The A_3 values of stress relaxation were obtained by the C-ring method and bent method and reported in the literature for type 316L and type 304 specimens as 0.6–1.8 ($\times 10^{-6}$/MPa/dpa). From these results, it was considered that the coefficient of austenitic stainless steel was not dependent on experimental method and the value was around 1.0 ($\times 10^{-6}$/MPa/dpa).

Acknowledgments

The authors would like to acknowledge staff members in the Department of the Japan Material Test Reactor (JMTR) and Department of Engineering Services in the Japan Atomic Energy Agency (JAEA) for carrying out the neutron irradiation and handling of specimens, and staff members of National Research Council Canada (NRC) and Atomic Energy Canada Ltd. (AECL) for handling and making precise neutron diffraction measurements of the highly active samples. In addition, some data were quoted from the Annual Report of the Japan Nuclear Energy Safety Organization (JNES) about the IASCC Project.

References

[1] K. Chatani, K. Takakura, M. Ando et al., in: 13th International Conference on Environmental Degradation of Materials in Nuclear Power Systems, 2007, P0091.
[2] S. Ooki, Y. Tanaka, K. Takamori et al., in: 12th International Conference on Environmental Degradation of Materials in Nuclear Power Systems – Water Reactors, 2005, p. 365.
[3] A. Jenssen et al., in: 11th International Conference on Environmental Degradation of Materials in Nuclear Power Systems – Water Reactors, 2003, p. 1015.
[4] P. Andresen et al., in: 11th International Conference on Environmental Degradation of Materials in Nuclear Power Systems – Water Reactors, 2003, p. 870.
[5] A.R. Causey, J. Nucl. Mater. 54 (1974) 64.
[6] A.R. Causey, J. Nucl. Mater. 98 (1981) 313.
[7] A.R. Causey, F.J. Butcher, S.A. Donohue, J. Nucl. Mater. 159 (1988) 101.
[8] A.R. Causey, G.J.C. Carpenter, S.R. MacEwen, J. Nucl. Mater. 90 (1980) 216.
[9] J.P. Foster, E.R. Gilbert, K. Bunde, D.L. Porter, J. Nucl. Mater. 252 (1998) 89.
[10] J.P. Foster, K. Bunde, M.L. Grossbeck, E.R. Gilbert, J. Nucl. Mater. 270 (1999) 357.
[11] J.P. Foster, K. Bunde, D.L. Porter, J. Nucl. Mater. 317 (1999) 167.
[12] Y. Ishiyama, K. Nakata, M. Obata et al., in: 11th International Conference on Environmental Degradation of Materials in Nuclear Power Systems – Water Reactors, 2003, p. 920.
[13] M. Obata, J.H. Root, Y. Ishiyama, et al., J. ASTM Int. 3 (1) (2006) JAI12348.
[14] R.J. Puigh, E.R. Gilbert, B.A. Chin, ASTM STP 782 (1982) 108.
[15] J. Nagakawa, J. Nucl. Mater. 212–215 (1994) 541.
[16] W.G. Wolfer, M. Ashkin, J. Appl. Phys. 47 (1976) 791.
[17] L.K. Mansur, Philos. Mag. A 39 (1979) 497.
[18] L.R. Greenwood, F.A. Garner, J. Nucl. Mater. 233–237 (1996) 1530.
[19] F.A. Garner, L.R. Greenwood, B.M. Oliver, Am. Soc. Test. Mater. (1999) p794.
[20] F.A. Garner, E.P. Simonen, B.M. Oliver, et al., J. Nucl. Mater. 356 (2006) 122.
[21] C.H. Woo, A. Garner, J. Nucl. Mater. 271–272 (1999) 78.
[22] F.A. Garner, M.B. Toloczko, M.L. Grossbeck, J. Nucl. Mater. 258–263 (1998) 1718.